Earthquake Research in China

Volume 27, Number 1, 2013

Landslides and Slope Fissures Triggered by the April 14, 2010 Yushu Earthquake, China[1]

Xu Chong, Xu Xiwei, and Yu Guihua

Key Laboratory of Active Tectonics and Volcano, Institute of Geology, CEA, Beijing 100029, China

On April 14, 2010 at 07:49 (Beijing time), a catastrophic earthquake with M_S 7.1 occurred at the central Qinghai-Tibetan Plateau. The epicenter was located at Yushu county, Qinghai Province, China. A total of 2036 landslides were determined from visual interpretation of aerial photographs and high resolution remote sensing images, and verified by selected field investigations. These landslides covered a total area of about 1.194km^2. Characteristics and failure mechanisms of these landslides are listed in this paper, including the fact that the spatial distribution of these landslides is controlled by co-seismic main surface fault ruptures. Most of the landslides were small scale, causing rather less hazards, and often occurring close to each other. The landslides were of various types, including mainly disrupted landslides and rock falls in shallows and also deep-seated landslides, liquefaction induced landslides, and compound landslides. In addition to strong ground shaking, which is the direct landslide triggering factor, geological, topographical, and human activity also have impact on the occurrence of earthquake triggered landslides. In this paper, five types of failure mechanisms related to the landslides are presented, namely, the excavated toes of slopes accompanied by strong ground shaking; surface water infiltration accompanied by strong ground shaking; co-seismic fault slipping accompanied by strong ground shaking; only strong ground shaking; and delayed occurrence of landslides due to snow melt or rainfall infiltration at sites where slopes were weakened by co-seismic ground shaking. Besides the main co-seismic surface ruptures, slope fissures were also delineated from visual interpretation of aerial photographs in high resolution. A total of 4814 slope fissures, with a total length up to 77.1km, were finally mapped. These slope fissures are mainly distributed on the slopes located at the southeastern end of the main co-seismic surface rupture zone, an area subject to strong compression during the earthquake.

Key words: Landslides triggered by the Yushu earthquake; Spatial distribution; Failure mechanism; Slope fissure

---

[1] Received on March 23, 2011; revised on September 29, 2011. This project was sponsored by the National Natural Science Foundation, China (40821160550).

INTRODUCTION

On April 14, 2010 at 07:49:40.7 (Beijing time), a catastrophic earthquake with M_S7.1 struck Yushu county, Qinghai Province, China. This earthquake is known as the Yushu earthquake. The earthquake registered a magnitude of M_S 7.1 (China Earthquake Networks Center, CENC) or M_W6.9 (U.S. Geological Survey, USGS, 2010). The epicenter is located at 33.1°N, 96.7°E with a focal depth of 33km according to CENC (it was later corrected to be located at 33.2°N, 96.6°E with a focal depth of 14km). Reports from USGS indicate that this earthquake occurred at April 13, 2010, 23:49:37 (UTC time), and its epicenter was located at 33.271°N, 96.629°E (±6.6km) with a focal depth of 10km (it was corrected to be located at 33.2°N, 96.6°E with a focal depth of 17km later). According to the bulletin of the Qinghai Earthquake Relief Headquarters, by 17:00, April 25, 2010, the earthquake had caused 2220 deaths, with 70 people missing, 12135 wounded (of which 1434 were seriously injured), and about 15000 houses collapsed. In this paper, an investigation is carried out on the spatial distribution of landslides triggered by the earthquake based on visual interpretation of high resolution remote sensing images and field investigations. Characteristics and failure mechanisms of the landslides are presented. An inventory of landslides triggered by the Yushu earthquake provides essential landslide data for subsequent seismic-induced landslide research, which is also produced in the GIS platform. Finally, slope fissures, together with the co-seismic main surface fault-ruptures triggered by the earthquake were delineated from visual interpretation of aerial photographs in high resolution.

1 SPATIAL DISTRIBUTION OF LANDSLIDES TRIGGERED BY THE YUSHU EARTHQUAKE

Earthquakes often trigger a large number of landslides, and earthquake event-based landslide inventories are an essential part of seismic-induced landslide research, such as spatial distribution analysis of landslides, susceptibility assessment, hazard assessment, risk assessment, and landform evaluation in earthquake stricken areas controlled by co-seismic landslides. Landslide inventories triggered by earthquakes are also constructed from visual interpretation of remote sensing images (aerial photographs or satellite images) and/or field investigations in recent years. For instance, landslides triggered by the 2008 Wenchuan earthquake attracted the attention of many geologists. Landslide inventories constructed by some researchers (Dai Fuchu et al., 2011; Gorum et al., 2011; Parker et al., 2011; Huang Runqiu and Li Weile, 2009; Xu Chong, 2012a; Xu Chong and Xu Xiwei, 2012a; Xu Chong et al., 2009a, 2009b, 2010a, 2013a) provide essential data for subsequent research (Xu Chong and Xu Xiwei, 2013a; Xu Chong et al., 2009c, 2010b, 2010c, 2010d; 2011a, 2011b, 2012a, 2012b, 2012c). Landslide inventories triggered by the 2010 Haiti earthquake (Xu Chong and Xu Xiwei, 2012b; Harp et al., 2011) were used for landslide spatial distribution analysis (Xu Chong and Xu Xiwei, 2012b) and landslide hazard assessment (Xu Chong et al., 2012d). Earlier results on the earthquake event related landslides include the M_W7.6 2005 Kashmir earthquake (Kamp et al., 2008; Owen et al., 2008), the 2004 Mid-Niigata earthquake (Yamagishi & Iwahashi, 2007; Sato et al., 2005), the 1999 M_W7.5 Chi-Chi earthquake (Wang et al., 2003; Khazai & Sitar, 2003), the 1994 M_W 6.7 Northridge earthquake (Harp & Jibson, 1996; Jibson & Harp, 1994; Parise & Jibson, 2000), the 1997 Umbria-Marche earthquake (Marzorati et al., 2002), the 1995 Hyogo-Ken earthquake (Fukuoka et al., 1997), the 1989 M_W 6.9 Loma Prieta earthquake (Keefer, 2000), the 1987 Ecuador earthquake (Tibaldi et al., 1995), the 23

November 1980 M_S6.9 Irpinia earthquake (Wasowski et al., 2002), the 1929 M7.7 Murchison earthquake (Pearce & O'Loughlin, 1985), and the 1811 New Madrid, Mo., earthquakes (Jibson & Keefer, 1989) etc. These publications provide plenty of inventories of earthquake event-based landslides for seismic landslide research.

The landslide inventory for landslides triggered by the Yushu earthquake was obtained from both visual interpretation of high resolution remote sensing images and field investigations. There were three steps for establishing the inventory: (1) creating landslide interpretation criteria and mapping an initial landslide inventory from visual interpretation of remote sensing images; (2) verifying some uncertain landslides by field investigation and revising the previous visual interpretation standards; (3) re-interpreting the images based on standards revised from field investigations and creating a final inventory of landslides triggered by the Yushu earthquake.

Remote sensing images used for visual interpretationof landslides are as follows: (1) true color aerial photographs in 0.2m and 0.4m resolutions flown by government agencies within several days after the earthquake; (2) panchromatic WorldView satellite images in 0.5m resolution after the earthquake; (3) multi-spectral SPOT 5 satellite images in 10m resolution, panchromatic SPOT 5 satellite images in 2.5m resolution before and after the earthquake.

Similar to the characteristics of images of landslides triggered by the 2008 Wenchuan earthquake (Dai Fuchu et al., 2011), landslides triggered by the Yushu earthquake in images have the following characteristics: (1) landslide deposits were clearly identified at the foot of the slopes, covering roads or other infrastructures, or extending into rivers or streams; (2) there is clearly no vegetation exposed on landslide slopes; (3) landslides have extremely bright white or dark brown contrast as compared to surrounding slopes; (4) debris movement paths of some landslides can be clearly observed. Individual landslide locations and boundaries can be delineated easily on these high resolution remote sensing images.

We follow the following principles to distinguish earthquake-triggered landslides from non-earthquake-triggered landslides: (1) landslides that can be found only on the images after the earthquake are earthquake triggered; (2) landslides that can be found in the images before the earthquake but cannot be found in the image after the earthquake are not regarded as earthquake triggered; (3) for landslides that can be found on both images before and after the earthquake, if the shapes of landslides are different, they are regarded to be triggered by the earthquake, otherwise, they are seen as pre-existing and are neglected.

Based on the GIS platform, the final spatial distribution map of landslides triggered by the 2010 Yushu earthquake was constructed (shown in Fig. 1). The result map shows that there were 2036 landslides triggered by the earthquake, with a total area of 1.194km^2 (Xu Chong et al., 2012e, 2013b). These landslides are distributed along a rectangular region with an area of about 1455.3km^2. The inventory was used for landslide spatial distribution analysis (Xu Chong and Xu Xiwei, 2012c; Xu et al., 2011c, 2012f), hazard assessment (Xu Chong, 2012b; Xu Chong and Xu Xiwei, 2012d, 2012e, 2012f; Xu Chong et al., 2012g), and quantitative studies on volume, gravitational potential energy reduction and the resultant regional centroid position change (Xu Chong and Xu Xiwei, 2013b) etc. The approximate center line of the rectangle is the main co-seismic surface rupture zone generated by the earthquake (Fig. 1). The three main co-seismic surface fault-ruptures are also shown on Fig. 1. The earthquake ruptured the Yushu County segment of the Garzê-Yushu fault and produced a 300°-striking, 65km-long surface rupture zone along the seismogenic fault. The surface rupture zone consists of the shear, transtensional, transpressional and extensional cracks, as well as mole tracks in right-stepovers or small pull-aparts in left-stepovers between en-echelon cracks with left-lateral component. The maximum left-lateral slip is 1.8m (Xu Xiwei et al., 2010; Chen Lichun et al., 2010; Zhang Junlong et al., 2010; Sun Xinzhe et al., 2010; Shi Feng et al., 2010).

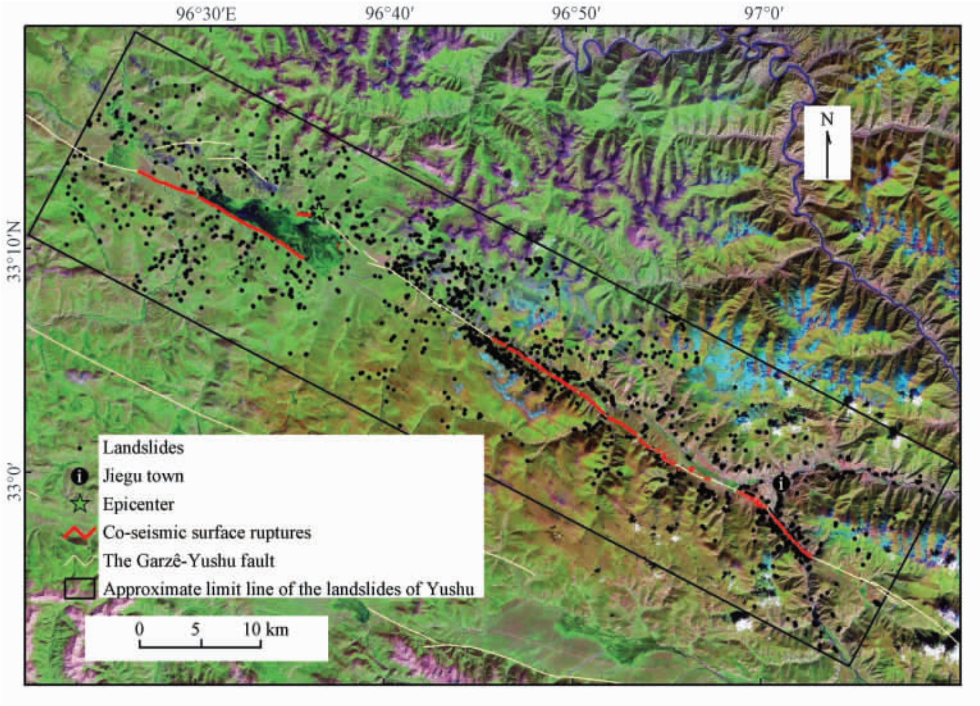

Fig. 1
Spatial distribution of landslides (black points) triggered by the Yushu earthquake

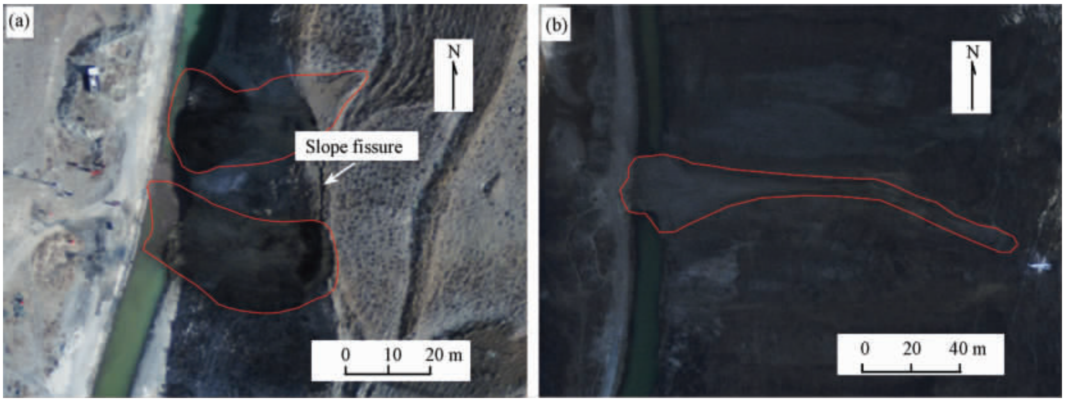

Fig. 2
Artificial canals were blocked by landslides triggered by the Yushu earthquake
(a) Two landslides blocked the canals; (b) A long-distance debris flow deposit blocked canals completely

2 CHARACTERISTICS OF THE LANDSLIDES

2.1 The Distribution of Landslides Is Strongly Controlled by the Main Co-seismic Surface Ruptures

As shown in Fig. 1, the 2 036 landslides are distributed in a rectangle region of 1455.3km^2. The approximate centerline of the rectangle shows the main co-seismic surface ruptures. The length of the rectangle (along the direction of extension of the surface rupture zone, or northwest direction) is about 76.75km and the width of the rectangle (perpendicular to the direction surface rupture, or northeast direction) is about 18.96km. Most of the landslides (1 082 landslides, amounting to 53% of the total landslide number, and with an area of 0.77km^2, accounting for 64.5% of the total landslide area) occurred about 2km from the main co-seismic surface ruptures. This indicates that the closer to the main co-seismic surface fault-ruptures, the more susceptible large landslides are.

2.2 *Most of the Landslides Are Small-sized and Caused Less Hazards*

The landform of the Yushu earthquake area is a gentle slope, which avoids blind areas on remote sensing images; vegetation is sparse; convenient traffic aids field investigations, and multi remote sensing images could have very high resolution (0.2m, 0.4m, and 0.5m etc.). These factors favored the delineation of landslides from visual interpretation of high resolution remote sensing images. Thus, even very small landslides (less than 1m in length) can be detected completely and in detail. 2 036 landslides triggered by the earthquake were found in the study area, with a total area of 1.194km^2. The average area of an individual landslide is 586.4m^2, which is much less than the average area of landslides triggered by the 2008 Wenchuan earthquake (Xu Chong, 2012a; Xu Chong et al., 2010a, 2013a; Dai Fuchu et al., 2011). Compared to landslides triggered by the 2008 Wenchuan earthquake (Yin Yueping, 2008; Xu Chong et al., 2009a, 2009b), no large or destructive landslides were triggered by the Yushu earthquake. Emergency investigation of the Yushu earthquake triggered landslides was organized by "Ministry of Land and Resources of the People's Republic of China" immediately after the earthquake (several days later). Report of emergency investigation on "the April 14" Yushu earthquake triggered geological hazards (Zhao Jiaxu et al., 2010) shows that the Yushu earthquake triggered landslides left 8 dead and 14 wounded, and caused a direct economic loss of about 600,000 Yuan (RMB) (Yin Yueping et al., 2010). Field investigations and visual interpretation of multi-source remote sensing images show that some of the landslides blocked roads and drainages, which however are small in scale. A few landslides partially dammed rivers. Fig.2(a) shows that two landslides partially blocked a canal, and formed a clear crack on the posterior slope in the middle of the two landslides. Fig.2(b) shows the long distance debris flow deposit, transferred from 140m away, blocking the canal completely.

2.3 *Landslides Were Generally Clustered in Spatial Distribution*

On some natural slopes, the landslides often occurred close to each other. As shown in Fig.3, on slopes around a low platform in the middle of the river, many landslides occurred on slopes in the eastern and southwestern directions.

2.4 *Types of Landslides Are Varied, Mainly in Rock Falls*

Landslides triggered by the Yushu earthquake include various types, mainly in rock falls and shallow, disrupted landslides, but also deep-seated landslides, liquefaction induced landslides, and compound landslides. Based on material movement types of the landslides, five types of landslides are classified roughly into two classes, which are rolling mode and slipping mode. Shallow, disrupted landslides and rock falls belong to the rolling mode. Deep-seated landslides and liquefaction induced landslides belong to the slipping mode. Compound landslides represent both the rolling mode and slipping mode. In the following sections, we will briefly discuss each type of based on field investigation and high-resolution remote sensing images analysis.

2.4.1 Rock Falls

Rock falls are individual boulders or disrupted masses of rock that descend along slopes by

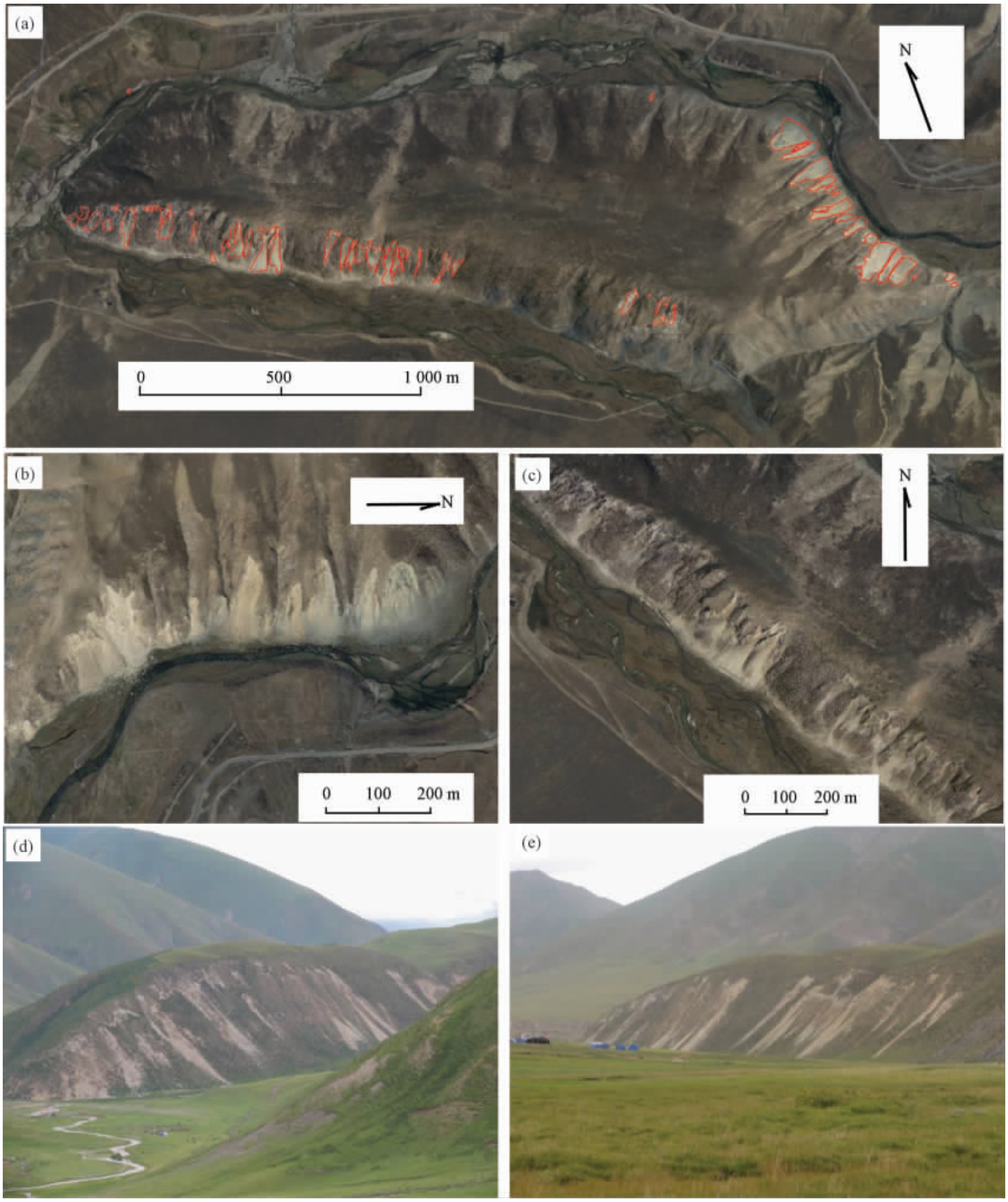

Fig. 3

Concentrated landslides occurred in the eastern and southwestern directions of slopes around a platform

(a) The overall view showing landslides occurring on slopes around a platform; (b) Image showing landslides occurring on slopes in the eastern direction; (c) Image showing landslides occurring on slopes in the southwestern direction; (d) Photo showing landslides on the western part of slopes in the southwestern direction; (e) Photo showing landslides on the eastern part of slopes in the southwestern direction bounding, rolling, or free fall, with the volume ranging generally from several cubic meters to a few tens of thousands of cubic meters (Keefer, 1984; Dai Fuchu et al., 2011). Among of the landslides, this type of landslide is the most common. They are mainly in the form of a rolling mode shallow landslide. Slope failures occur along weak structural planes under strong ground shaking, and the landslide materials roll down and accumulate at the foot of slopes. The deposits are seriously crushed and gravel size generally ranges from 20cm to 30cm in diameter. Fig. 4 shows images or photos of some rock falls triggered by the earthquake. Most of such landslides occurred in the colluvial layer. Fig. 4(a) and (b) show rock falls in limestone occurring at the outlet of western bank of a gully, and the diameter of the biggest rock is about 0.8m (Institute of Geology, China Earthquake Administration, 2010). Fig. 4(c) shows a shallow rock fall occurring in the loose deposit layer of a riverside slope. Fig. 4(d) shows rock falls 700m west of Longhongda village.

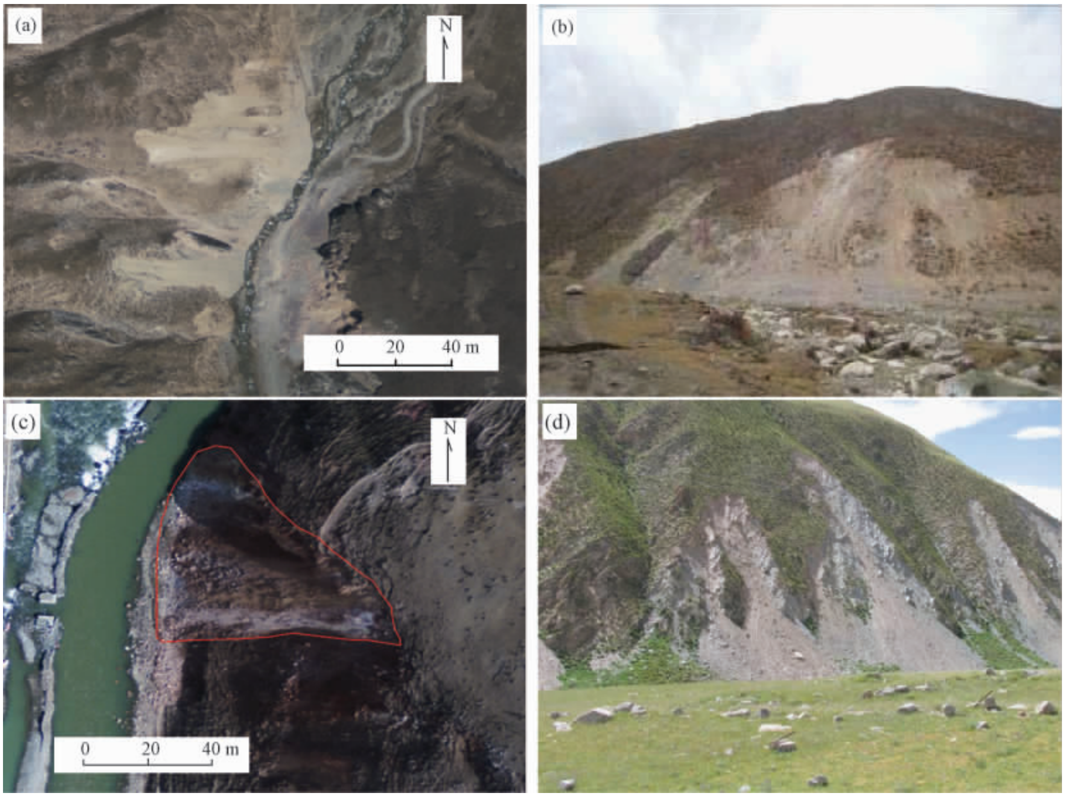

Fig. 4

Collapse-type landslides

(a) Rock falls and the deposits reaching the riverside; (b) Photo showing the rock falls of image A (Institute of Geology, China Earthquake Administration, 2010); (c) Shallow rock fall occurring in the loose deposit layer; (d) Rock falls occurring 700m west of Longhongda village

2.4.2 Deep-seated Landslides

Among the 2 036 landslides, deep-seated landslides are much lower in number than shallow disrupted landslides or rock falls. The depth of the deep-seated landslides is commonly thicker than the shallow disrupted ones in similar areas. The movement distances of the deep-seated landslides are generally short and are slipping mode. Fig. 5(a) shows a small-scale, deep-seated landslide. The vegetation on the deposits is better maintained, which shows a complete sliding or slipping movement mode. From Fig. 5 (b), we see that the depth of deep-seated landslides is thicker than the shallow disrupted ones and rock falls, and the scarp along the landslide crown is rather steep.

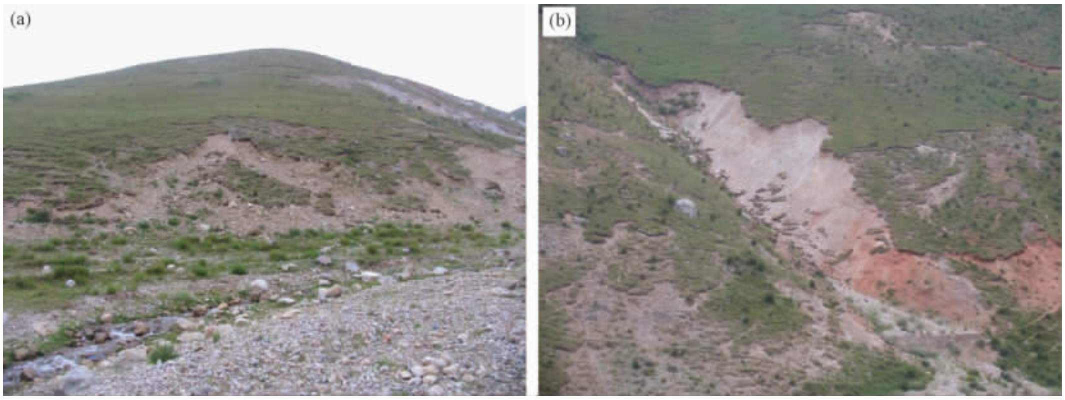

Fig. 5

Landslides of sliding type

(a) A small-scale, deep-seated landslide of complete slipping mode; (b) A small-scale, deep-seated landslide with steep scarp along the landslide crown

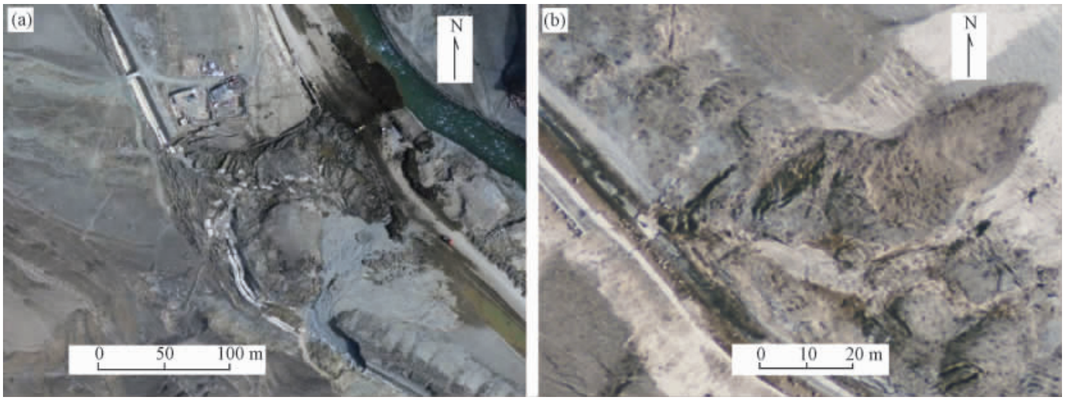

Fig. 6

Flow-slip landslides

(a) A flow-slip landslide destroying artificial canals and roads; (b) Another flow-slip landslide destroying artificial canals

2.4.3 Flow-slip Landslides

Liquefaction induced landslides are strongly affected by water liquefaction. The liquefaction induced landslides are commonly larger, slowly sliding with flow slipping or creep slipping and are of soil landslides. These landslides may destroy roads and canals. Fig. 6 shows images of two liquefaction induced landslides. Fig. 6 (a) (32°58′1″N, 97°1′20″E) shows a liquefaction induced landslide destroying canals and roads. The front of the landslide reached the river, causing local waterfalls in the river. Another liquefaction induced landslide (32°58′30″N, 97°0′48″E) destroyed canals, as shown in Fig. 6 (b).

2.4.4 Shallow Disrupted Landslides

Shallow and disrupted landslides generally occurred as rock falls during the 2010 Yushu earthquake. The material movement mode of this type of landslide is similar to rock falls of slipping mode. The characteristics of shallow disrupted landslides include crushed landslide materials, small (the majority of gravels are between 10cm and 15cm in diameter) deposit gravels, long movement distances, a clear and narrow traveling path, similar to the movement, accumulation and shape of debris flow. Fig. 7 shows two photos of shallow disrupted landslides. Fig. 7 (a) shows a group of shallow disrupted landslides, rather similar to rock falls. It is classified as shallow disrupted landslide type due to its broken accumulation materials, small gravel, and clearly identifiable movement path. Fig. 7 (b) shows a landslide occurring from the slope ridge and accumulating at the foot of the slopes. Narrow movement paths can be clearly observed and identified. Both the movement mode and shape of accumulation area of shallow disrupted landslides are similar to debris flows.

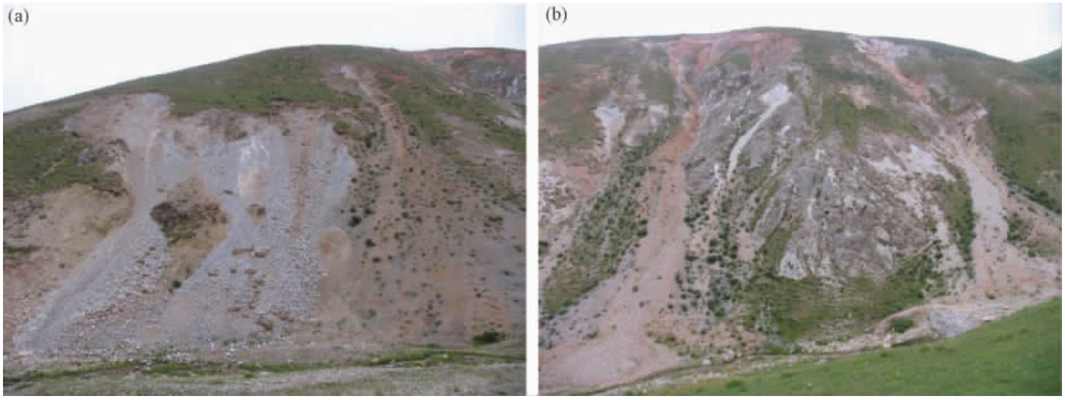

Fig. 7

Photos of debris-flow landslides

(a) The debris-flow landslide on the hillside; (b) A debris-flow landslide occurring from movement of narrow valley

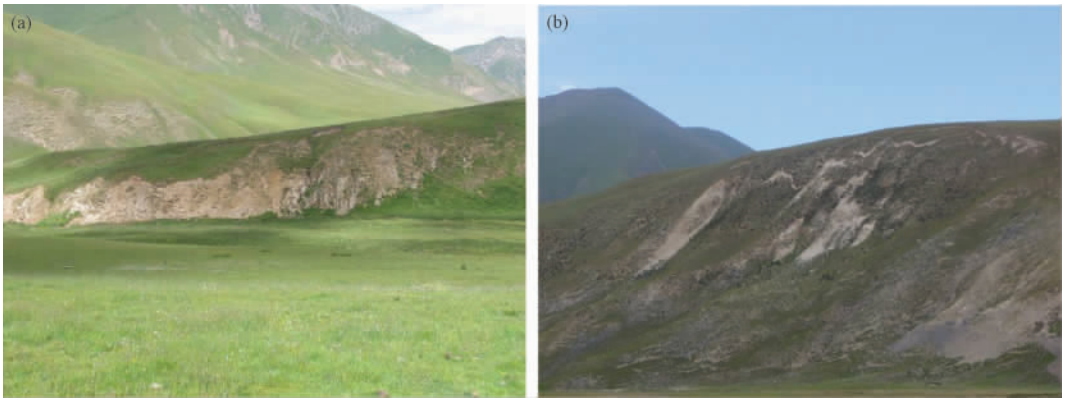

Fig. 8

Two photos of typical compound landslides

(a) Rock falls occurring at the foot of the slope and slope fissures on top of these rock falls; (b) Shallow disrupted landslides occurring on the middle of the slope and several cracks at the trailing edge of the landslide

In general, compound landslides are composed of deep-seated landslides and shallow disrupted landslides or rock falls. Shallow disrupted landslides or rock falls occurred at the front or middle of the slope. On the edge or trailing edge of the slopes, several tensile fissures can be noted. This indicates that the integrity of the slope has been destroyed during the earthquake. Fig. 8 shows two photos of typical compound landslides. The compound landslide, as shown in Fig. 8 (a), indicates that rock falls clustered at the foot and front of the slope and there are clear fissures at the scarp along the landslide crown. Fig. 8 (b) shows a compound landslide which is composed of a deep-seated landslide and several shallow disrupted landslides. These shallow disrupted landslides occurred on the middle of the slope. Several fissures can be clearly observed at the trailing edge of the deep-seated landslide. Rainfall infiltration into the fissures may result in overall sliding, thus generating a new disaster.

3 FAILURE MECHANISMS OF LANDSLIDES TRIGGERED BY THE YUSHU EARTHQUAKE

Strong ground shaking is a dynamic trigger for generating earthquake-triggered landslides. However, the failure mechanisms of earthquake triggered landslides also include factors such as lithology, geological structure, slope gradient, and human activity, etc. In the following sections, based on field investigation and remote sensing image analysis, five failure mechanisms are introduced. They are: excavated slope toes accompanied by strong ground shaking; surface water infiltration accompanied by strong ground shaking; co-seismic fault slipping accompanied by strong ground shaking; only strong ground shaking; delayed occurrence of landslides due to snow melting or rainfall infiltration at sites where slopes were weakened by the co-seismic strong ground shaking.

3.1 Excavated Slope Toes with Strong Ground Shaking

In general, landslides due to excavation of slope toes with strong ground shaking occur on the uphill of the excavated projects, such as construction of roads and canals. During road and canal construction, slope toe excavation is the most common engineering work, which may disturb the stability of natural slopes and alter the stress state of the slopes, resulting in stress concentration at toes of slopes and reducing sliding resistance. Thus, the slopes are prone to landslides accompanied by strong ground shaking during an earthquake. Some landslides of this type occurred on the uphill side of roads and canals during the 2010 Yushu earthquake. Generally, landslides of this type among the 2036 landslides are often small in scale, with a short running distance. The landslides may block roads or canals. Although low hazards, the landslide debris deposits may accumulate on roads or in manmade canals and need to be cleared in time. Landslide deposits may block the manmade canals, causing water infiltration and resulting in downhill slope instability which will lead to sliding or slope creep due to liquefaction. Fig. 9 shows a group of landslides caused by the excavation of slope toes and strong ground shaking. Fig. 9 (a) indicates a landslide which occurred on the upslope of a road. The loose accumulation layers of road upslopes were destroyed by strong ground shaking and excavation at the toes of slopes. The landslide in Fig. 9 (b) is located at 32°57′43″N, 97°01′39″E, which is an example of a landslide caused by canal excavation and strong ground shaking. There is only 60m from the trailing edge of the landslide to the co-seismic main surface ruptures. The canal was blocked by the landslide deposits. There are several slope fissures developed at the trailing edge of the landslide. It shows that the whole natural slope was deformed during the earthquake. Landslides are most likely to occur again on the slopes under conditions of rainfall or snow melt infiltration. So, appropriate control measures should be taken to prevent secondary hazards.

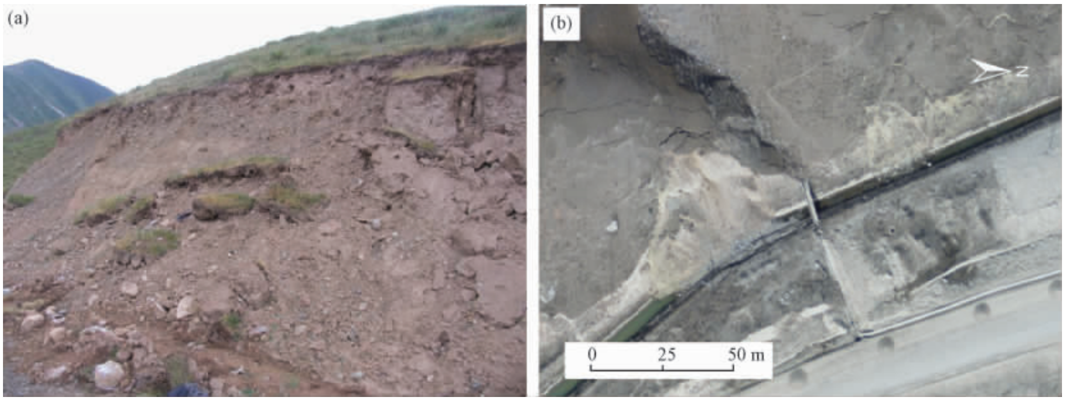

Fig. 9

Landslides caused by slope toe excavation and strong ground shaking

(a) Photo of landslides occurring on road upslope; (b) Image of landslides occurring on a canal's upslope

3.2 Surface Water Infiltration Accompanied by Strong Ground Shaking

Among of the landslides triggered by the Yushu earthquake, there are several landslides caused by surface water infiltration into slope fissures triggered by strong ground shaking. In general, this kind of landslide occurs on the downslope of artificial canals. Strong ground shaking during the Yushu earthquake produced a lot of slope fissures and water infiltration might occur because of these slope fissures. The natural slopes were liquefied under the effect of water infiltration and strong ground shaking, and resulted in landsliding in the forms of creep slip and flow. Such landslides may block roads, will continue during the forthcoming rainy season. Fig. 10 shows a group of this type of landslide. The landslide in Fig. 10 (a) is located at 32°58′24″N, 97°0′58″E, which blocked roads. There is clear, dark, water-saturated debris on the upper slope. Fig. 10 (b) shows two landslides of this type located close to each other at 32°58′39″N, 97°0′41″E. Both of the landslides partly blocked roads. Landslides caused by this failure mechanism generally correspond with the liquefaction induced landslides discussed in section 3.4.

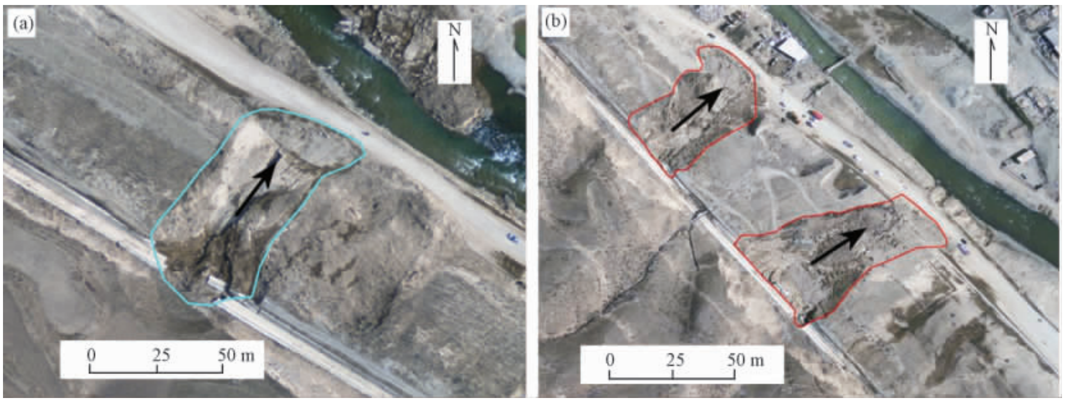

Fig. 10

Earthquake-triggered landslides caused by surface water infiltration

(a) A typical landslide caused by surface water infiltration and ground shaking;
(b) Two landslides that partly blocked the roads

3.3 Co-seismic Fault Slipping Accompanied by Strong Ground Shaking

Landslides caused by co-seismic fault slip and strong ground shaking mean the landslides crossed by co-seismic main surface ruptures. During the earthquake, structures of slopes crossed by seismogenic faults may be destroyed by slip of the seismic fault. As can be found, there is clear evidence of the co-seismic main surface ruptures crossing the front or rear of the slopes where landslides occurred. In this case, landslides often occur during strong ground shaking. Fig. 11 shows two landslides crossed by co-seismic surface ruptures. The mass movement types of these two landslides are rolling (shown in Fig. 11(a) and 11(b)) and slipping (shown in Fig. 11(c) and 11(d)), respectively. Fig. 11(a) shows a rock fall occurring near the largest coseismic slip displacement. The aerial photograph of the landslide and spatial distribution of coseismic main surface ruptures by field investigation indicate that the landslide is crossed by the seismogenic fault (Fig. 11(b)). In the northwestern and southeastern directions of the landslide, clear dextral co-seismic surface ruptures can be observed. The materials movement mode is rolling, as revealed by the photo (Fig. 11(a)). Fig. 11(c) and 11(d) show another landslide caused by co-seismic fault slipping and strong ground shaking in slipping mode.

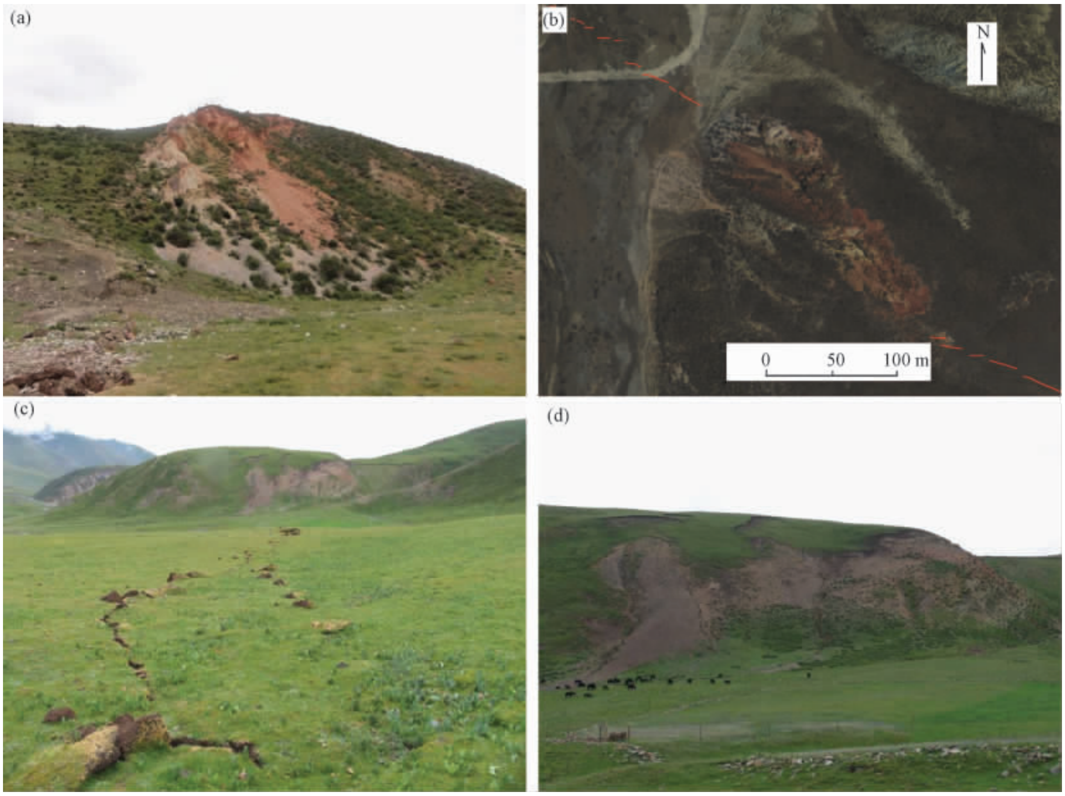

Fig. 11

Earthquake-triggered landslides caused by fault slipping

(a) A rock fall occurring near the largest co-seismic slip displacement; (b) Aerial photograph of the rock fall crossed by the co-seismic surface ruptures; (c) Perspective of a landslide crossed by co-seismic surface ruptures; (d) Close-range of a landslide crossed by the main co-seismic surface ruptures

3.4 *Landslide Caused Merely by Strong Ground Shaking*

It is most common for landslides to occur on natural slopes during earthquakes. Landslides of this type are caused by strong ground shaking, which is an external factor. Lithology, rock structure, and slope gradient etc. are internal factors affecting this type of landslide. Fig. 12 shows several landslides of this type in dense distribution. Fig. 12 (a), (b), (c), and (d) are photos of landslides (located at 33°0′45″N, 97°4′34″E) occurring on slopes near the Longhongda village caused by strong ground shaking. Fig. 12 (e) shows several rock falls numbered No. 1, No. 2, No. 3 and No. 4 near Zhisong village, east of Yushu county. Volumes of the four landslides are about 5 000m^3, 2 500m^3, 500m^3 and 100m^3, respectively. Fig. 12 (f) shows a landslide (located at 32°57′3″N, 97°2′2″E) that blocked roads near Sangka village, at the south of Yushu county, and its volume is about 3 000m^3.

3.5 *Landslide Caused by Snowmelt or Rain Infiltration on Slopes That Experienced Strong Ground Shaking*

Landslides of snow melt or rain infiltration type on slopes that experienced strong ground shaking mainly occurred near ridges and upper slopes. High elevation and steep slope angle are the characteristics of such slopes. In winter, snow accumulates on the ridges and upper slopes throughout the Yushu earthquake stricken region for high elevation and cold weather. Meadows on the slopes cracked under the effect of strong ground shaking and topographic ground shaking amplification. When summer comes, the infiltration of melting snow or rain fall will result in many shallow landslides occurring along the roots of the meadows. Landslides of this type often show a dendritic shape in large area, even covering the entire slope. Generally, depths of landslides of this type are less than 0.5m. Photos (taken in August, 2010) of Fig. 13 show that landslides occurred on ridges of two slopes induced by melting snow or rainfall on slopes that had experienced strong ground shaking. These landslides did not occur immediately after the Yushu earthquake, but a long time after the earthquake under conditions of rainfall infiltration or melting snow. So, strictly speaking, although affected by strong ground shaking, landslides of this type are triggered by snow melting or rainfall infiltration later. These landslides are excluded in the inventory map of landslides triggered by the 2010 Yushu earthquake. In general, these landslides are far away from human settlements and engineering construction in the Yushu earthquake stricken regions. Although these landslides did not have much impact on the safety of human life and property, they could destroy the vegetation on ridges and upper slopes, affecting to a certain extent the already vulnerable ecological environment of the plateau.

4 SLOPE FISSURES TRIGGERED BY THE EARTHQUAKE

In addition to the mainco-seismic surface ruptures along the Garzê-Yushu fault, many slope fissures have also occurred and been delineated from visual interpretation of aerial photographs in high resolution of 0.2m and 0.4m, and verified by selected field checks. Most of the slope fissures are distributed in the northern direction of Yushu county. Fig. 14 shows a group of photos of typical slope fissures caused by the earthquake, which indicate that the slope structures suffered slight damage. These slope fissures occurred due to strong ground motion, deformation, and gravity. Based on the aerial photographs, 4 814 slope fissures were mapped (Fig. 15), with a total length of 77.1 km. These slope fissures are mainly distributed on the slopes located at the southeastern end of the main co-seismic surface fault-ruptures, which is an area of turning part and termination of the seismogenic fault and the stress accumulation zone before the earthquake occurrence. The accumulated stress was released during the earthquake and resulted in deformation and slope fissures on the slopes. Fig. 16 shows area that slope fissures densely

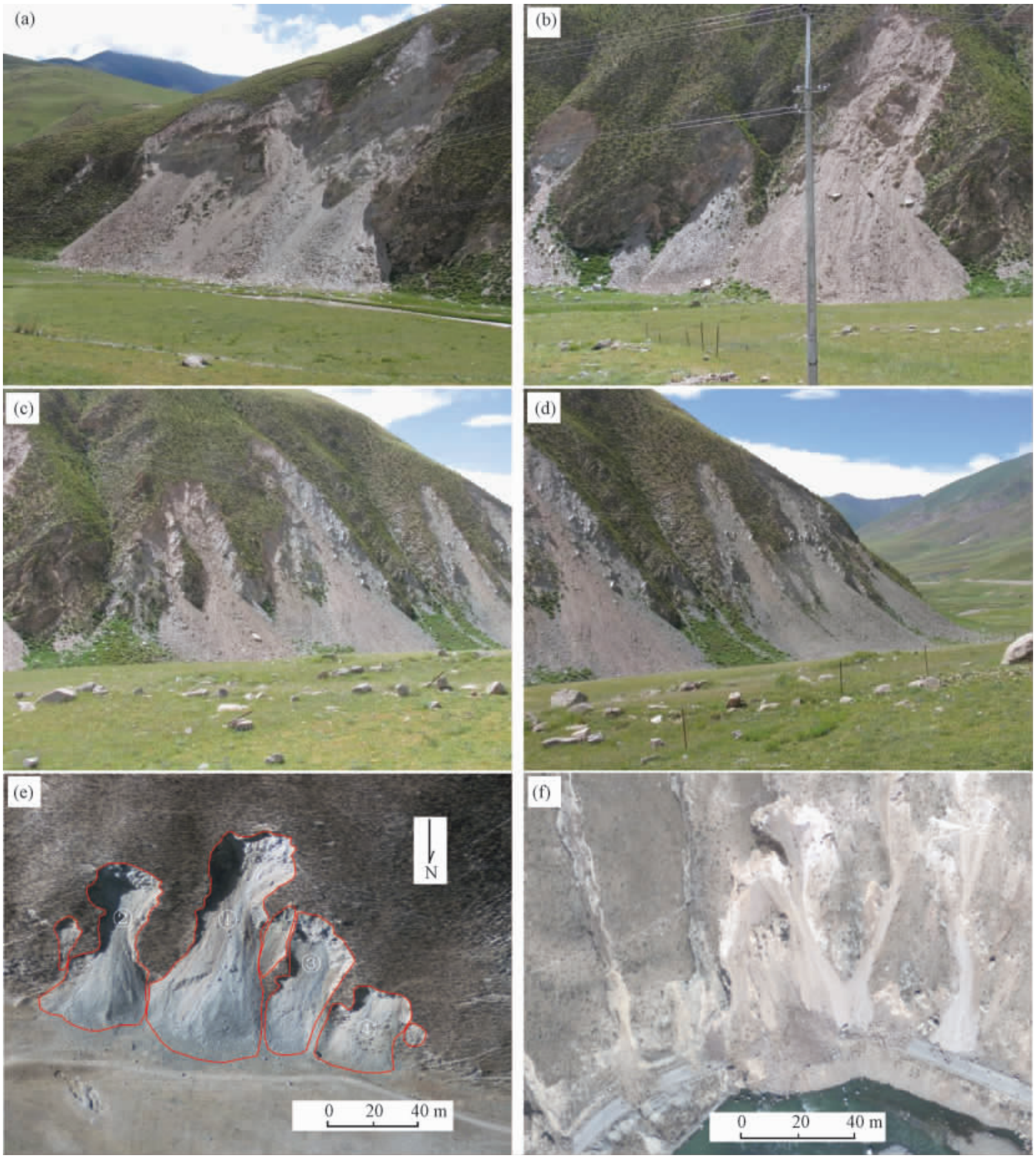

Fig. 12

Earthquak-triggered landslides caused by shaking

Photos of landslides (a), (b), (c) and (d) occurring on slopes near Longhongda village caused by ground shaking; (e) Landslides occurring near Zhisong village, east of Yushu county; (f) Landslides near Sangka village, south of Yushu county, which blocked the road

occurred. It can be observed that most of the slope fissures occurred along the co-seismic main surface fault-ruptures. It shows asymmetric distribution of slope fissures along the main co-seismic fault-ruptures. Most of the slope fissures occurred on slopes in the southwestern part of the main fault-ruptures. There are two reasons as follows: (1) Because the seismogenic fault of the Yushu earthquake is of sinistral strike-slip type, the southwestern wall of the southeastern end of the fault underwent compressive stress, whereas the southwestern wall was subject to tensile stress. Slope

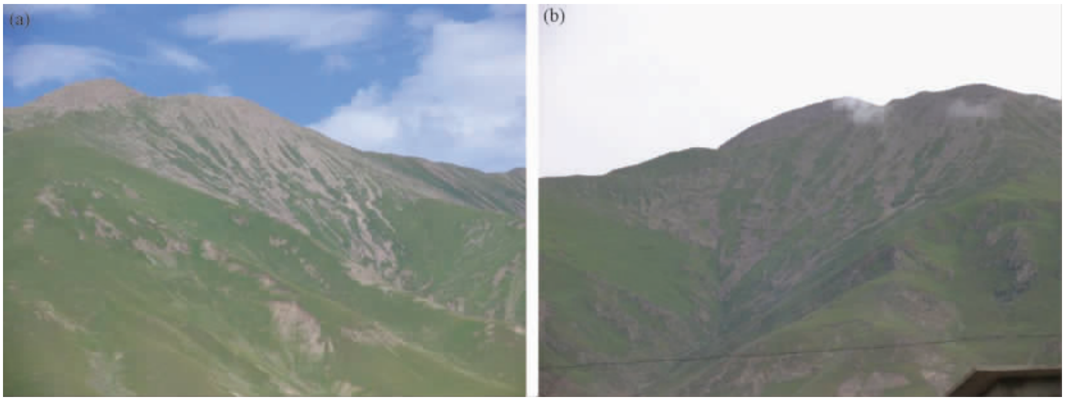

Fig. 13

Photos taken in August, 2010 landslides caused by snow melting or rain fall after the earthquake

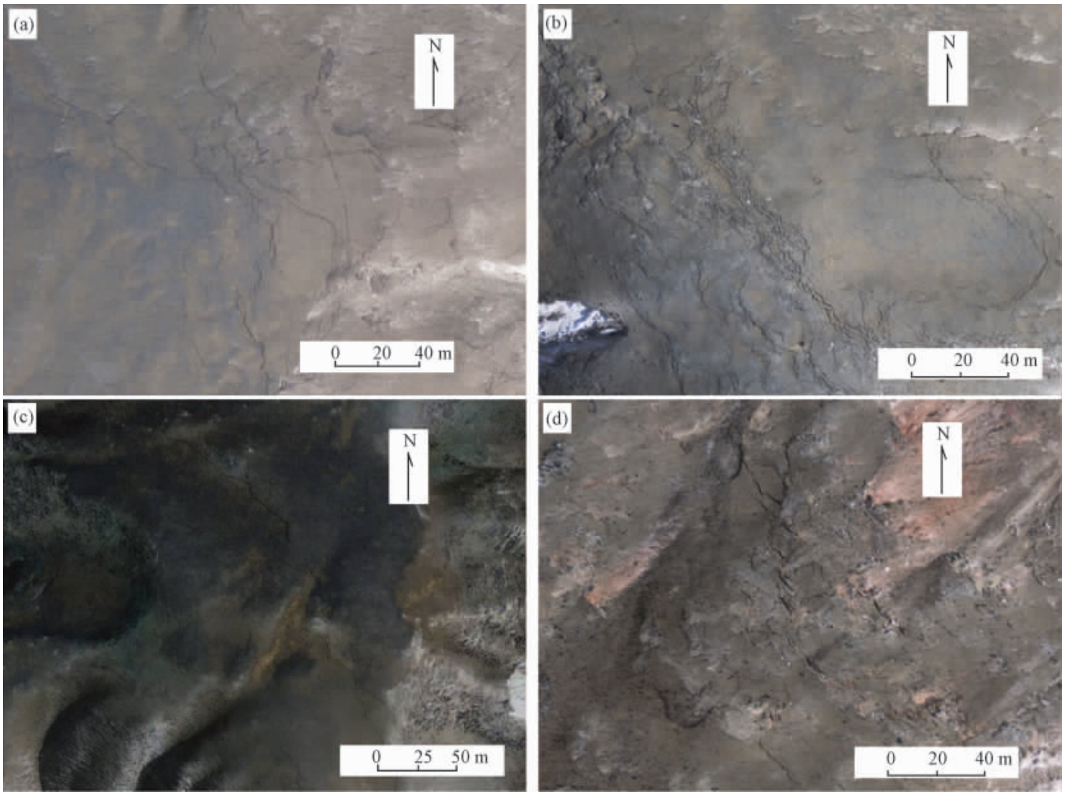

Fig. 14

Typical aerial photographs of slope fissures triggered by the Yushu earthquake

fissures commonly occurred on the southwestern wall of the southeastern end of the fault. (2) The slope fissures are concentrated at areas (Fig. 15) located at the turning part of the co-seismic surface ruptures, which have characteristics similar to thrust faults. The southwestern side of the fault is the hanging wall and the northeastern side is the footwall. The geometric characteristics of the co-seismic main surface ruptures are similar to the Liupanshan fault located at the eastern section of the Haiyuan fault, Ningxia Hui Autonomous Region, China (Burchfiel et al., 1991;

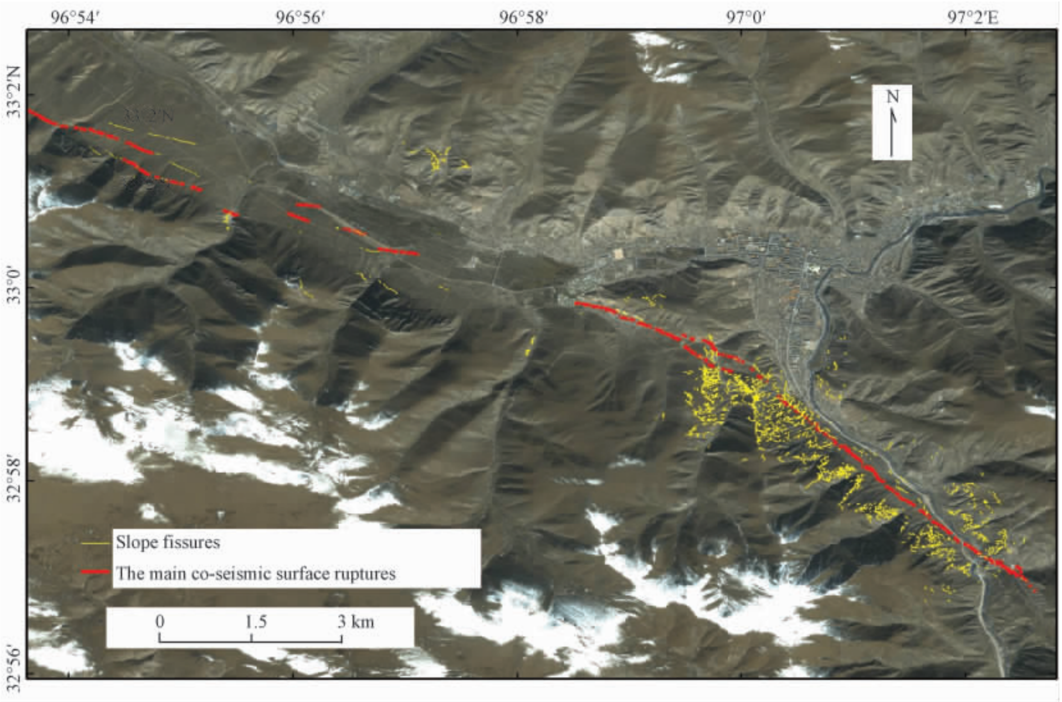

Fig. 15
Spatial distribution of slope fissures triggered by the Yushu earthquake

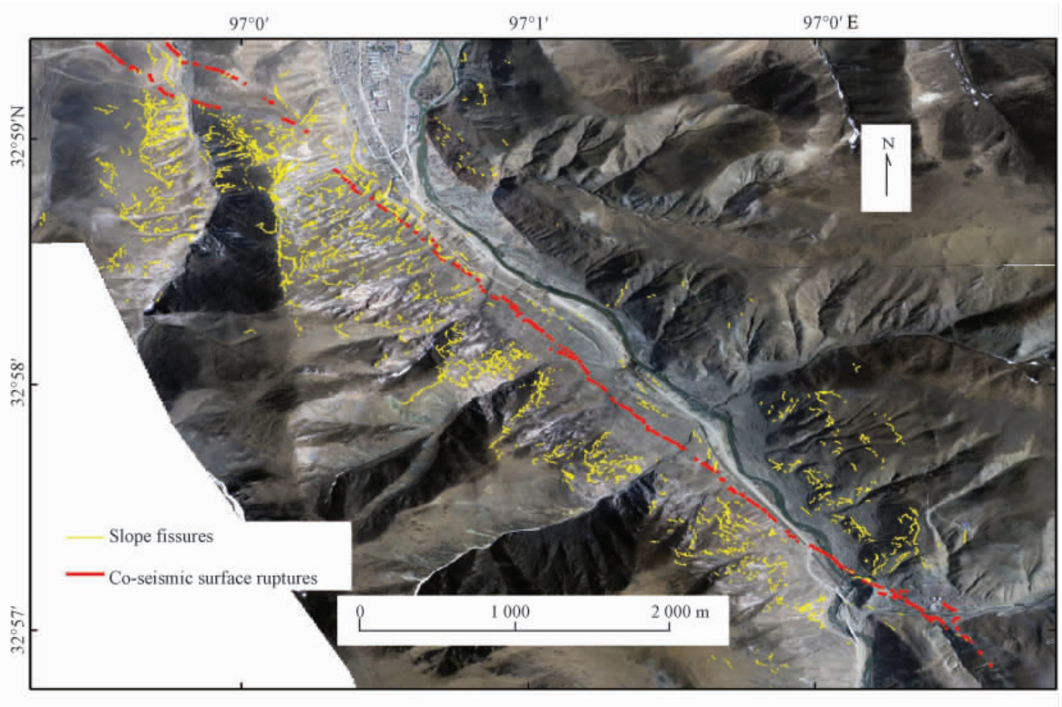

Fig. 16
Local spatial distribution characteristics of the slope fissures triggered by the Yushu earthquake

Institute of Geology, China Seismological Bureau and Seismological Bureau of Ningxia Hui Autonomous Region, 1990). As we know, hazards caused by thrust faults generally generate earthquakes much larger than that of strike-slip faults. It is necessary to carry out more in-depth scientific research on the mechanisms to determine why the slope fissures densely occurred in these areas.

5 ANALYSIS AND DISCUSSIONS

The 2008 Wenchuan earthquake occurred at the eastern boundary of the Bayan Har block and the Longmenshan fault was the seismogenic fault, whereas the 2010 Yushu earthquake occurred at the middle of the southern boundary of the Bayan Har block. Although both of the strong earthquakes occurred at the boundary of the Bayan Har block, landslides triggered by the 2008 Wenchuan earthquake (Xu Chong et al., 2010a) are much more serious than landslides triggered by the 2010 Yushu earthquake, in landslide number, scale, distribution area, subsequent disasters etc. Several possible reasons are listed as follows:

(1) Difference of earthquake magnitudes. Both earthquakes belong to shallow earthquakes. According to the China Earthquake Networks Center, the magnitude of the Wenchuan earthquake is $M_S 8.0$, and the magnitude of the Yushu earthquake is $M_S 7.1$. Based on the formula of earthquake magnitude and released energy, $\lg E = 11.8 + 1.5M$, where E means released energy, M represents earthquake magnitude. The energy released by the Wenchuan earthquake is about 22.387 times greater than the Yushu earthquake.

(2) Difference in slip behavior of the seismogenic faults. The seismogenic fault of the Wenchuan earthquake is the Longmenshan thrust fault with right-lateral slip movement. The strike of the fault plane is approximately northeast. The seismogenic fault of the Yushu earthquake, named the Yushu-Garzê fault, is a section of the Xianshuihe fault belt with left-lateral slip. As we know, earthquakes generated by thrust faults are more devastating than earthquakes generated by strike-slip faults in similar magnitude. In addition, there is a significant "hanging wall effect" of thrust fault, which may cause serious hazards, that is, the landslides on the hanging wall will be larger in number, scale, and spatial distribution area than that of footwall. Thus, more serious disasters may be caused on the hanging wall. However there is no such effect with strike-slip fault type earthquakes.

(3) Difference of slope angles between the stricken areas of the two earthquakes. Slopes in steep terrain are expected to have high frequency of landslides because of generally higher shear stresses associated with high gradients. Besides, steep slopes can also amplify the effect of seismic waves. The region hit by the Yushu earthquake is mainly high altitude, low slope gradient mountains, with slope gradients between 0° and 30°, whereas the slope gradient range is generally from 20° to 50° in the Wenchuan earthquake stricken area. The average slope gradient of the Wenchuan earthquake area is much higher than that of the Yushu earthquake area.

(4) Different location of epicenters. The epicenter of the Yushu earthquake is located at the center of the Qinghai-Tibetan Plateau, where the elevation difference is small in the Yushu earthquake stricken area, while the epicenter of the Wenchuan earthquake is located at the Longmenshan Mountains. The Longmenshan fault, located at the eastern boundary of the Qinghai-Tibetan Plateau, the junction of the Qinghai-Tibetan Plateau and the South China Block, is the seismogenic fault, where the elevation difference is larger. Thus, different locations of epicenters of the two earthquakes result in great differences of landslides triggered by the two earthquakes.

(5) Difference of precipitation between the two earthquake-stricken areas. Water can reduce slope stability, thus making the slopes prone to landslide. The annual precipitation of Yushu County is about 487mm, whereas the annual precipitations of most of the counties or cities in areas stricken by the Wenchuan earthquake is more than 700mm, such as the Mianzhu,

Dujiangyan, Pingwu, Beichuan, Shifang, and Qingchuan counties or cities etc. (in addition to the Maoxian and Wenchuan counties). Among these counties and cities hit by the Wenchuan earthquake, Beichuan county has the highest annual precipitation, which is 1300mm, and Dujiangyan city ranks second, with 1 174mm (Meteorological Bureau of Sichuan Province, 2008). Therefore, the annual precipitation of the Wenchuan earthquake stricken area is about twice to three times the Yushu earthquake area. This is possibly one of the reasons why the hazards caused by the Wenchuan earthquake-triggered landslides are much more serious than those of the Yushu earthquake.

Landslides triggered by the 2010 Yushu earthquake are mainly in small scale, and the areas stricken by the earthquake are in a plateau area, where the population is sparse. Therefore, hazards to settlements and environments caused by the co-seismic landslides of the 2010 Yushu earthquake are much lower than the 2008 Wenchuan earthquake.

6 CONCLUSIONS

(1) Spatial distribution maps of landslides triggered by the 2010 Yushu earthquake were constructed based on field investigations and visual interpretation of multi-source high resolution remote sensing images. The maps show that a total of 2 036 landslides were triggered by the earthquake, with a total area of 1.194km^2. These landslides are distributed in an approximately rectangular region of 1 455.3km^2 approximately along the central line of co-seismic main surface ruptures.

(2) The characteristics of the landslides triggered by the Yushu earthquake are as follows: the landslides were strongly controlled by co-seismic main surface ruptures and occurred close to each other. Most of the landslides are small in scale and caused slight hazards. The landslide types are varied, mainly of shallow disrupted landslide and rock fall, also including deep-seated landslides, liquefaction induced landslides, and compound landslides.

(3) There are five failure mechanisms for the landslides, including excavated slope toes accompanied by strong ground shaking; surface water infiltration accompanied by strong ground shaking; co-seismic fault slip accompanied by strong ground shaking; merely strong ground shaking; delayed occurrence of landslides due to snow melt or rainfall infiltration at sites where slopes were weakened by co-seismic ground shaking

(4) Slope fissures triggered by the Yushu earthquake were also interpreted and delineated from aerial photographs inhigh resolution. A total of 4 814 slope fissures, with a total length of 77.1km, excluding the main surface ruptures, were mapped. These fissures are mainly distributed on the slopes located at the southeastern end of the main co-seismic surface ruptures, an area subject to strong compression during the earthquake.

(5) Compared to landslides triggered by the 2008 Wenchuan earthquake, landslides triggered by the Yushu earthquake are much less in number, small in scale, and caused slighter hazards. We conclude that there are possibly five reasons for the differences: earthquake magnitude; slip behavior of seismogenic faults; slope gradients in areas stricken by the two earthquakes; difference in location setting of the epicenters; and difference in precipitation between the earthquake-hit areas.

ACKNOWLEDGEMENTS

This research is supported by the National Natural Science Foundation of China (41202235), the Basic Scientific Fund of the Institute of Geology, China Earthquake Administration (IGCEA1215). The authors would like to express their sincere gratitude to Li Xiaoli, Cheng Jia, Sun Xinzhe, Liu Huaguo, Wang Hu, Yao Shenghai, and Li Zhimin et al., for their assistance in the field investigation of landslides triggered by the Yushu earthquake.

This paper has been published in Chinese in the journal of *Seismology and Geology*, Volume 34, Number 1, 2012.

REFERENCES

Burchfiel B. C, Zhang Peizhen, Wang Yipeng, et al. Geology of the Haiyuan fault zone, Ningxia Hui Autonomous Region, China, and its relation to the evolution of the northeastern margin of the Tibetan Plateau [J]. *Tectonics*, 1991, 10(6): 1091 ~ 1110.

Chen Lichun, Wang Hu, Ran Yongkang, et al. The M_S7.1 Yushu earthquake surface rupture and large historical earthquakes on the Garzê-Yushu Fault [J]. *Chinese Science Bulletin*, 2010, 55(13): 1200 ~ 1205 (in Chinese with English abstract).

Dai Fuchu, Xu Chong, Yao Xin, et al. Spatial distribution of landslides triggered by the 2008 M_S8.0 Wenchuan earthquake, China [J]. *Journal of Asian Earth Sciences*, 2011, 40(4): 883 ~ 895.

Fukuoka H, Sassa K, Scarascia-Mugnozza G. Distribution of landslides triggered by the 1995 Hyogo-Ken Nanbu earthquake and long runout mechanism of the Takarazuka Golf Course landslide [J]. *Journal of Physics of the Earth*, 1997, 45(2):83 ~ 90.

Gorum T, Fan Xuanmei, van Westen CJ, et al. Distribution pattern of earthquake-induced landslides triggered by the 12 May 2008 Wenchuan earthquake [J]. *Geomorphology*, 2011, 133(3 ~ 4): 152 ~ 167.

Harp EL, Jibson RW, Dart RL. The effect of complex fault rupture on the distribution of landslides triggered by the 12 January 2010, Haiti earthquake [C]. *Proceedings of the Second World Landslide Forum*, Rome: October 3 ~ 7, 2011, 5 pages.

Harp E L, Jibson R W. Landslides triggered by the 1994 Northridge, California, earthquake [J]. *Bulletin of the Seismological Society of America*, 1996, 86(1B):S319 ~ S332

Huang Runqiu, Li Weile. Analysis of the geo-hazards triggered by the 12 May 2008 Wenchuan earthquake, China [J]. *Bulletin of Engineering Geology and the Environment*, 2009, 68(3): 363 ~ 371.

Institute of Geology, China Seismological Bureau, Seismological Bureau of Ningxia Hui Autonomous Region. *Haiyuan Active Fault Belt* [M]. Beijing: Seismological Press, 1990. 286 (in Chinese).

Institute of Geology, Chinese Earthquake Administration. *Investigation Report of Surface Ruptures and Geological Hazards Triggered by Yushu M_S 7.1 Earthquake* [EB/OL]. 2010, http://www.eq-igl.ac.cn/html/8a834a81158a15aa01158a1bbbd40003/_content/10_04/26/1272249728202.html (in Chinese).

Jibson R W, Harp E L. Landslides triggered by the Northridge earthquake [J]. *Earthquake & Volcanoes*, 1994, 25(1): 31 ~ 41.

Jibson R W, Keefer D K. Statistical analysis of factors affecting landslide distribution in the new Madrid seismic zone, Tennessee and Kentucky [J]. *Engineering Geology*, 1989, 27(1 - 4): 509 ~ 542.

Kamp U, Growley B J, Khattak G A, et al. GIS-based landslide susceptibility mapping for the 2005 Kashmir earthquake region [J]. *Geomorphology*, 2008, 101(4): 631 ~ 642.

Keefer D K. Landslides caused by earthquakes [J]. *Geological Society of America Bulletin*, 1984, 95(4): 406 ~ 421.

Keefer D K. Statistical analysis of an earthquake-induced landslide distribution — The 1989 Loma Prieta, California event [J]. *Engineering Geology*, 2000, 58(3 - 4): 231 ~ 249.

Khazai B, Sitar N. Evaluation of factors controlling earthquake-induced landslides caused by Chi-Chi earthquake and comparison with the Northridge and Loma Prieta events [J]. *Engineering Geology*, 2003, 71(1 - 2): 79 ~ 95.

Marzorati S, Luzi L, Amicis MD. Rock falls induced by earthquakes: A statistical approach [J]. *Soil Dynamics and Earthquake Engineering*, 2002, 22(7): 565 ~ 577

Meteorological Bureau of Sichuan Province. *Rainfall Climatic Characteristics in Serious Area Stricken by "5.12" Wenchuan Big Earthquake in Sichuan Province* [EB/OL]. 2008, http://www.scqx.gov.cn/qxkp/qxkj/2008090515400077.html (in Chinese).

Owen L A, Kamp U, Khattak G A, et al. Landslides triggered by the 8 October 2005 Kashmir earthquake [J]. *Geomorphology*, 2008, 94(1 ~ 2): 1 ~ 9.

Parise M, Jibson R W. A seismic landslide susceptibility rating of geologic units based on analysis of characteristics of landslides triggered by the 17 January, 1994 Northridge, California earthquake [J]. *Engineering Geology*, 2000, 58(3 ~ 4): 51 ~ 270.

Parker R N, Densmore A L, Rosser N J, et al. Mass wasting triggered by 2008 Wenchuan earthquake is greater than orogenic growth [J]. *Nature Geoscience*, 2011, 4(7): 449~452.

Pearce A J, O'Loughlin C L. Landsliding during an *M*7.7 earthquake: Influence of geology and topography [J]. *Geology*, 1985, 13(12): 855~858.

Sato H P, Sekiguchi T, Kojiroi R, et al. Overlaying landslides distribution on the earthquake source, geological and topographical data: the Mid Niigata prefecture earthquake in 2004, Japan [J]. *Landslides*, 2005, 2(2): 143~152.

Shi Feng, He Honglin, Zhang Ying. Remote sensing interpretation of the M_S7.1 Yushu earthquake surface ruptures [J]. *Technology for Earthquake Disaster Prevention*, 2010, 5(2): 220~227 (in Chinese with English abstract).

Sun Xinzhe, Xu Xiwei, Chen Lichun, et al. Characteristics of surface rupture of the M_S7.1 Yushu, Qinghai Province earthquake at two representative places [J]. *Seismology and Geology*, 2010, 32(2): 338~344 (in Chinese with English abstract).

Tibaldi A, Ferrari L, Pasquare G. Landslides triggered by earthquakes and their relations with faults and mountain slope geometry: An example from Ecuador [J]. *Geomorphology*, 1995, 11(3): 215~226.

U.S. Geological Survey. *Advanced National Seismic System (ANSS), Shake Map, Global Region, Maps of Ground Shaking and Intensity for Event* 2010 *yr, Southern Qinghai, China* [EB/OL]. 2010, http://earthquake.usgs.gov/eqcenter/shakemap (in Chinese).

Wang W N, Wu H L, Nakamura H, et al. Mass movements caused by recent tectonic activity: The 1999 Chi-Chi earthquake in central Taiwan [J]. *The Island Arc*, 2003, 12(4): 325~334.

Wasowski J, Gaudio V D, Pierri P, et al. Factors controlling seismic susceptibility of the Sele Valley slopes: The case of the 1980 Irpinia earthquake re-examined [J]. *Surveys in Geophysics*, 2002, 23(6): 563~593.

Xu Chong, Dai Fuchu, Chen Jian, et al. Identification and analysis of secondary geological hazards triggered by a magnitude 8.0 Wenchuan earthquake [J]. *Journal of Remote Sensing*, 2009a, 13(4): 745~762 (in two versions of Chinese and English).

Xu Chong, Dai Fuchu, Xiao Jianzhang. Statistical analysis of the characteristic parameters of landslides triggered by the May 12, 2008 Wenchuan earthquake [J]. *Journal of Natural Disasters*, 2011a, 20(4): 147~153 (in Chinese with English abstract).

Xu Chong, Dai Fuchu, Xu Xiwei, et al. GIS-based support vector machine modeling of earthquake-triggered landslide susceptibility in the Jianjiang River watershed, China [J]. *Geomorphology*, 2012a, 145~146: 70~80.

Xu Chong, Dai Fuchu, Xu Xiwei. Earthquake triggered landslide susceptibility evaluation based on GIS platform and weight-of-evidence modeling [J]. *Earth Science—Journal of China University of Geosciences*, 2011b, 36(6):1155~1164 (in Chinese with English abstract).

Xu Chong, Dai Fuchu, Xu Xiwei. Wenchuan earthquake-induced landslides: An overview [J]. *Geological Review*, 2010a, 56(6): 860~874 (in Chinese with English abstract).

Xu Chong, Dai Fuchu, Yao Xin, et al. GIS based certainty factor analysis of landslide triggering factors in Wenchuan earthquake of 12 May 2008, Sichuan, China [J]. *Chinese Journal of Rock Mechanics and Engineering*, 2010b, 29(S1): 2972~2981 (in Chinese with English abstract).

Xu Chong, Dai Fuchu, Yao Xin, et al. GIS-based landslide susceptibility assessment using analytical hierarchy process (AHP) for May 12, 2008 Wenchuan earthquake region [J]. *Chinese Journal of Rock Mechanics and Engineering*, 2009c, 28(S2): 3978~3985 (in Chinese with English abstract).

Xu Chong, Dai Fuchu, Yao Xin, et al. Study on the distribution of landslides triggered by the May 12, 2008 Wenchuan earthquake in two square typical regions [J]. *Journal of the Graduate School of the Chinese Academy of Sciences*, 2010c, 27(5): 621~631 (in Chinese with English abstract).

Xu Chong, Dai Fuchu, Yao Xin, et al. Study on Wenchuan earthquake-induced landslide susceptibility evaluation based on GIS platform and certainty factor analysis method [J]. *Journal of Engineering Geology*, 2010d, 18(1): 15~26 (in Chinese with English abstract).

Xu Chong, Dai Fuchu, Yao Xin. Incidence number and affected area of Wenchuan earthquake-induced landslides [J]. *Science & Technology Review*, 2009b, 27(11): 79~81 (in Chinese with English abstract).

Xu Chong, Xu Xiwei, Dai Fuchu, et al. Analysis of spatial distribution and controlling parameters of landsides triggered by the April 14, 2010 Yushu earthquake [J]. *Journal of Engineering Geology*, 2011c, 19(4): 505~510 (in Chinese with English abstract).

Xu Chong, Xu Xiwei, Dai Fuchu, et al. Comparison of different models for susceptibility mapping of earthquake triggered landslides related with the 2008 Wenchuan earthquake in China [J]. *Computers & Geosciences*, 2012b, 46: 317 ~ 329.

Xu Chong, Xu Xiwei, Dai Fuchu, et al. Landslide hazard mapping using GIS and weight of evidence model in Qingshui river watershed of 2008 Wenchuan earthquake struck region [J]. *Journal of Earth Science*, 2012c, 23(1): 97 ~ 120.

Xu Chong, Xu Xiwei, Lee YH. The 2010 Yushu earthquake triggered landslide hazard mapping using GIS and weight of evidence modeling [J]. *Environmental Earth Sciences*, 2012g, 66(6): 1603 ~ 1616.

Xu Chong, Xu Xiwei, Wu Xiyan, et al. Detailed landslide inventories triggered by the 2008 Wenchuan earthquake and their spatial distribution statistical analyses [J]. *Journal of Engineering Geology*, 2013a, 20(1): (in Chinese with English abstract) (in press).

Xu Chong, Xu Xiwei, Yu Guihua, et al. Susceptibility analysis of impact factors of landslides triggered by Yushu earthquake [J]. *Science & Technology Review*, 2012f, 30(1): 18 ~ 24 (in Chinese with English abstract).

Xu Chong, Xu Xiwei, Yu Guihua. Earthquake triggered landslide hazard mapping and validation related with the 2010 Port-au-Prince, Haiti earthquake [J]. *Disaster Advances*, 2012d, 5(4): 1297 ~ 1304.

Xu Chong, Xu Xiwei, Yu Guihua. Landslides triggered by slipping-fault-generated earthquake on a plateau: An example of the 14 April 2010, M_S 7.1, Yushu, China earthquake [J]. *Landslides*, 2013b, Online. doi: 10.1007/s10346-012-0340-x

Xu Chong, Xu Xiwei, Yu Guihua. Study on the characteristics, mechanism, and spatial distribution of Yushu earthquake triggered landslides [J]. *Seismology and Geology*, 2012e, 34(1): 47 ~ 62 (in Chinese with English abstract).

Xu Chong, Xu Xiwei. Application of logistic regression model and its validation for Yushu earthquake triggered landslide hazard mapping [J]. *Journal of Engineering Geology*, 2012e, 20(3): 326 ~ 333 (in Chinese with English abstract).

Xu Chong, Xu Xiwei. Comment on "spatial distribution analysis of landslides triggered by 2008.5.12 Wenchuan Earthquake, China" by Shengwen Qi, Qiang Xu, Hengxing Lan, Bing Zhang, Jianyou Liu [Engineering Geology 116 (2010) 95 ~ 108] [J]. *Engineering Geology*, 2012a, 133 ~ 134: 40 ~ 42.

Xu Chong, Xu Xiwei. Controlling parameter analyses and hazard mapping for earthquake triggered-landslides: An example from a square region in Beichuan county, Sichuan Province, China [J]. *Arabian Journal of Geosciences*, 2013a, Online. doi:10.1007/s12517-012-0646-y

Xu Chong, Xu Xiwei. GIS and ANN model for earthquake triggered landslides susceptibility zonation [J]. *Geological Science and Technology Information*, 2012d, 31(3): 116 ~ 121 (in Chinese with English abstract).

Xu Chong, Xu Xiwei. Quantitative study on volume, gravitational potential energy reduction and caused regional centroid position change: An example of the 2010 Yushu earthquake triggered landslides [J]. *Science & Technology Review*, 2013b, 31(1): 5 ~ 13 (in Chinese with English abstract).

Xu Chong, Xu Xiwei. Spatial distribution difference of landslides triggered by slip-fault type earthquake on two sides of the fault [J]. *Geological Bulletin of China*, 2012c, 31(4): 532 ~ 540 (in Chinese with English abstract).

Xu Chong, Xu Xiwei. Spatial distribution of seismic landslides and their erosion thickness related with a transpressional fault caused earthquake of subduction zone [J]. *Journal of Engineering Geology*, 2012b, 20(5): 732 ~ 744 (in Chinese with English abstract).

Xu Chong, Xu Xiwei. The 2010 Yushu earthquake triggered landslides spatial prediction models based on several kernel function types [J]. *Chinese Journal of Geophysics*, 2012f, 55(9): 2994 ~ 3005 (in Chinese with English abstract).

Xu Chong. Detailed inventory of the 2008 Wenchuan earthquake triggered landslides and its comparison with global other earthquake events [J]. *Science & Technology Review*, 2012a, 30(25): 18 ~ 26 (in Chinese with English abstract).

Xu Chong. Seismogenic structure of Yushu earthquake and preliminary earthquake-induced landslide hazard evaluation [J]. *Engineering Geological Computer Applications*, 2012b, (1): 1 ~ 14 (in Chinese with English abstract).

Xu Xiwei, Yu Guihua, Sun Xinzhe. *Yushu Earthquake Slip: Implication of Great Earthquake Migration along Boundary Fault System of Bayan Har Block, Tibetan Plateau* [C]. American Geophysical Union, Fall Meeting 2010, 2010, abstract #T22A-04.

Yamagishi H, Iwahashi J. Comparison between the two triggered landslides in Mid-Niigata, Japan by July 13 heavy rainfall and October 23 intensive earthquakes in 2004 [J]. *Landslides*, 2007, 4(4): 389 ~ 397.

Yin Yueping, Zhang Yongshuang, Ma Yinsheng, et al. Research on major characteristics of geohazards induced by the Yushu M_S 7.1 earthquake [J]. *Journal of Engineering Geology*, 2010, 18(3): 289 ~ 296 (in Chinese with English abstract).

Yin Yueping. Research on the geo-hazards triggered by Wenchuan earthquake, Sichuan [J]. *Journal of Engineering Geology*, 2008, 16(4): 433 ~ 444 (in Chinese with English abstract).

Zhang Junlong, Chen Changyun, Hu Chaozhong, et al. Surface rupture and coseismic displacement of the Yushu M_S7.1 earthquake, China [J]. *Earthquake*, 2010, 30(3): 1 ~ 12 (in Chinese with English abstract).

Zhao Jiaxu, Li Yujun, Zhang Lizheng, et al. *Report of Emergency Investigation on* "4.14" *Yushu Earthquake Triggered Geological Hazards* [R]. The Qinghai Geological Environment Monitoring Station, Xining City, Qinghai Province, 2010 (in Chinese).

About the Author

Xu Chong, born in 1982, is an associate research professor at the Institute of Geology, China Earthquake Administration. He received his Ph. D. from the Institute of Geology and Geophysics, Chinese Academy of Sciences in 2010. His current research interests include earthquake triggered landslides, active faults, and landform evolutions in earthquake zones. E-mail: xc11111111@126.com, xuchong@ies.ac.cn

Xu Xiwei (corresponding author), born in 1962, is a research professor, and works at the Institute of Geology, China Earthquake Administration. E-mail: xiweixu@vip.sina.com